Available online at www.sciencedirect.com
SCIENCE DIRECT®
ELSEVIER
International Journal of Solids and Structures 42 (2005) 3794–3806
INTERNATIONAL JOURNAL OF SOLIDS and STRUCTURES
www.elsevier.com/locate/ijsolstr

A study on the relief of residual stresses in weldments with explosive treatment

Jinxiang Zhang [a], Kaishin Liu [a,*], Kai Zhao [a], Xiaojie Li [b], Ying Liu [a], Kai Zhang [b]

[a] *State Key Laboratory for Turbulence and Complex Systems and Department of Mechanics and Engineering Science, Peking University, 5 Yiheyuan Road, Beijing 100871, P.R. China*
[b] *State Key Laboratory of SAIE, Dalian University of Technology, Dalian 116024, P.R. China*

Received 7 August 2004; received in revised form 29 November 2004
Available online 21 January 2005

Abstract

Explosive treatment is an efficient and economical technique in reducing welding residual stresses. The whole course of residual stress reduction is investigated both numerically and experimentally, in order to discover the mechanism of the explosive treatment and optimizing the technique. It is proved that the reflection and superposition of stress waves aroused by explosive loading lead to redistribution and remarkable reduction of welding residual stresses. Moreover, the optimum working conditions, such as detonator shape, width, location, explosive loading and velocities, are also discussed. The numerical results and the experimental ones are in reasonable agreement with each other.

Keywords: Welding; Residual stress; Explosive treatment; Numerical simulation; Experiments

1. Introduction

Welding is a reliable and efficient metal-joining method widely used in industry. During the course of welding, residual stresses are commonly produced near the weld line, owing to the intensely heating and cooling (Masubuchi, 1980). Tensile residual stresses may increase the rate of damage by fatigue or creep, and reduce the load capacity. Compressive residual stresses are generally beneficial, but cause a decrease in the allowable buckling load. Therefore, Huseby (1958), Lin and Chou (1995), Yang and Lee (1997)

* Corresponding author. Tel.: +86 10 62765844; fax: +86 10 62751812.
E-mail address: kliu@mech.pke.edu.cn (K. Liu).

0020-7683/$ - see front matter
doi:10.1016/j.ijsolstr.2004.11.017

and Lu et al. (1998), have reported plenty of methods to reduce welding residual stresses. However, these techniques may be difficult to apply due to limited access to the affected areas or extremely hazardous work environment. Explosive treatment is a new technique. It reduces residual stresses by producing a controlled explosive loading through welded joints. The technique is the groundwork for an American patent (Holtzman, 1966) and a Japanese patent (Horioka, 1978). Schmidt and Shockey (1992) studied the reduction of residual stresses in weldments with explosive treatment experimentally. Actually, the technique had been successfully adopted in some practices (Chadwick, 1971; Kudinov and Petushkov, 1984; Shida et al., 1986). These studies and applications show that the explosive treatment has a bright future because its low expense, simple operation, and universal application, especially for large-sized structures. However, the mechanism of this technique is still unclear.

This paper aims to study the mechanism of explosive treatment by researching on the whole variation processes of residual stress and strain fields. For the requirement of this work, a thermal stress analysis should be executed in advance to obtain the initial residual stress and strain fields after welding. Then, the dynamic behavior of the weldment under explosive loading is analyzed, especially the wave motion and its effect upon residual stresses and strains. Several work conditions of explosive technique are studied for optimizing the technique. Then, an engineering practice of explosive treatment is reported and the experimental results are compared with the numerical ones.

2. Fundamental equations of the problem

An indirect iterative method (Tall, 1964) is used to study the cooling process through welding, in which the heat transfer and stress analysis have been decoupled and been solved independently. The transient temperature field obtained from thermal analysis is stored at each step and used as an internal force to the latter stress analysis.

2.1. Temperature field analysis

The three-dimensional transient heat conductive equation without interior heat source is written as

$$\rho c(T)\frac{\partial T}{\partial t}-\frac{\partial}{\partial x}\left(K_x(T)\frac{\partial T}{\partial x}\right)-\frac{\partial}{\partial y}\left(K_y(T)\frac{\partial T}{\partial y}\right)-\frac{\partial}{\partial z}\left(K_z(T)\frac{\partial T}{\partial z}\right)=0 \tag{1}$$

where T is temperature, ρ the density of material, $c(T)$ the specific heat, t the time. $K_x(T)$, $K_y(T)$ and $K_z(T)$ are conductive coefficients along x, y and z directions, respectively. The heat boundary conditions are given by

$$T=\overline{T}\quad(\text{on boundary }\mathbf{\Gamma}_1) \tag{2}$$

$$K_x(T)\frac{\partial T}{\partial x}n_x+K_y(T)\frac{\partial T}{\partial y}n_y+K_z(T)\frac{\partial T}{\partial z}n_z=h(T)(T-T_0)\quad(\text{on boundary }\mathbf{\Gamma}_2) \tag{3}$$

where n_i are the cosines of outward normal vectors, $h(T)$ is the heat diffusion coefficient on boundary $\mathbf{\Gamma}_2$, $\overline{T}=\overline{T}(\mathbf{\Gamma}_1,t)$ the temperature at boundary $\mathbf{\Gamma}_1$, in which $\mathbf{\Gamma}_1$ is the boundary of weld line, $\mathbf{\Gamma}_2$ the boundary of the plate. For isotropic material, $K_x(T)=K_y(T)=K_z(T)=K(T)$. Parameters $c(T)$, $h(T)$, and $K(T)$ are variables of temperature. The initial heat conditions are

$$\overline{T}=T_0(\text{for plate})\quad\overline{T}=T_1(\text{for weld line})\quad(t=0) \tag{4}$$

where T_0 is the room temperature, T_1 the initial temperature of the weld line.

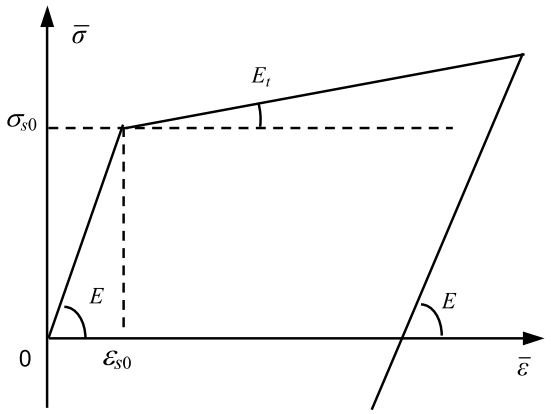

Fig. 1. Bilinear isotropic elastoplastic model.

2.2. Stress field analysis

Stress analysis are used in both generation and reduction process of residual stresses. The fundamental equations of stress field analysis are as follows:

Equation of motion

$$\sigma_{ij,j} = \rho u_{i,tt} \tag{5}$$

Geometric equation

$$\varepsilon_{ij} = \frac{1}{2}(u_{i,j} + u_{j,i}) \tag{6}$$

Constitutive equation

$$\sigma_{ij} = D_{ijkl}(\varepsilon_{kl} - \varepsilon^T_{kl}) \tag{7.1}$$

$$\sigma_{ij} = \sigma_{s0}(\dot{\varepsilon}_{ij}) + E_{\mathrm{h}}\varepsilon^{\mathrm{ep}}_{ij} \tag{7.2}$$

where σ_{ij} and ε_{ij} are the stress and strain components, u_i the displacement components, D_{ijkl} the elasto-plastic constants, σ_{s0} the yield stress. "," denotes the derivative with respect to the subscript variable. $\varepsilon^{\mathrm{ep}}_{ij} = \sqrt{\frac{2}{3}\varepsilon^{\mathrm{p}}_{ij}\varepsilon^{\mathrm{p}}_{ij}}$ are the equivalent plastic strain components, in which $\varepsilon^{\mathrm{p}}_{ij}$ are components of plastic strain. Parameter E_{h} is given in terms of Young's modulus E and tangent modulus E_{t} by $E_{\mathrm{h}} = \frac{EE_{\mathrm{t}}}{E-E_{\mathrm{t}}}$.

The constitutive Eqs. (7.1) and (7.2) are for same material in different loading conditions. Eq. (7.1) is for the elasto-plastic thermal stress analysis in the welding cooling process, in which a bilinear isotropic hardening model (see Fig. 1) is adopted. The effect of temperature on the mechanical properties is considered, but the effect of strain rate is unconsidered since it is very slight. On the other hand, the strain rate effect, but not the temperature effect, is taken into account in Eq. (7.2), which is for the dynamic loading analysis in the course of residual stress relieving, because the intensive loading fleets the plate so fast that the effect of temperature could be neglected.

3. Numerical analysis

Consider a butt-welded steel plate as shown in Fig. 2. The dimension of the model is 400 mm × 300 mm × 16 mm, including a weld line of 12 mm width. Half of the Finite Element model is

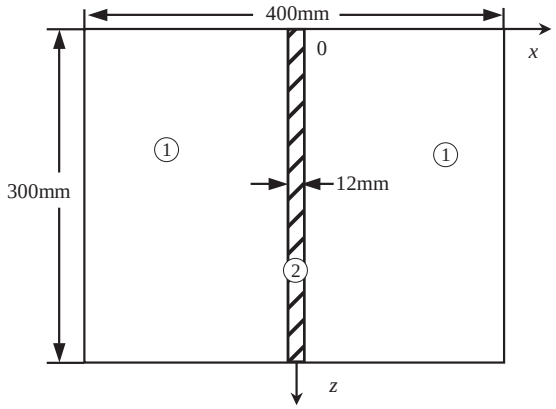

Fig. 2. The butt-welded plate. (① steel plate, ② weld line).

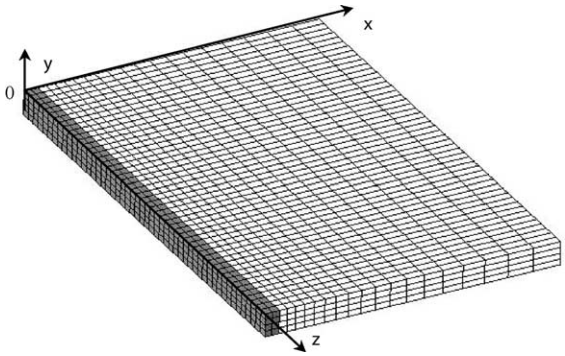

Fig. 3. The numerical model. (Half of the plate is taken, the shadow region represents the weld line).

used, according to the characteristic of symmetry. The model consists of two parts: the steel plate and the weld line, the latter is along z direction. Considering the demands of both accuracy and efficiency, non-uniform elements are utilized in element divisions. The nearer the distance from the weld line, the smaller the elements. The minimum element length is 1 mm, while the maximum one is 10 mm. In other directions, the element sizes are uniformly taken as 1 mm. The model totally includes 60 000 elements and 69 309 nodes. The sketch map of the element discretization is shown in Fig. 3. Hexahedral solid isoparametric elements are adopted in descretization and the Galerkin weighted residuals formulation is used to discrete the governing equation.

In this study, both the plate and the weld line are made of 16 MnR steel. Its composition is 0.19% C, 0.45% Si, 0.023% P, 0.015% S and 1.4% Mn. The temperature-dependent material properties used in the cooling course are shown in Table 1 (Editorial board, 1995), corresponding to Eq. (7.1). Material properties used in the relieving course are taken as the value at 20 °C in Table 1, and the rate-dependent parameter $\sigma_{s0}(\dot{\varepsilon}_{ij})$ are presented in Table 2 (Shi and Yu, 1996) in detail, based on Eq. (7.2).

3.1. Forming of residual stresses

The initial temperature of the weld line T_1 is assigned to 800 °C. Variable time steps, from 0.001 s to 1 s, are adopted in the calculation, since the temperature drops down rapidly at the beginning and then slowly

Table 1
Mechanical and thermal properties of 16 MnR steel

Temperature T (°C)	20	100	300	500	600	800
Elastic modules $E(T)$ (GPa)	210	205	185	165	120	100
Tangent modules $E_t(T)$ (GPa)	4.6	4.2	3.8	2.5	2.0	0.5
Yield stress $\sigma_{s0}(T)$ (MPa)	345	312	283	233	140	90
Thermal expansion coefficient $\alpha(T)$ ($\times 10^{-6}$/°C)	8	8.31	12.31	13.71	13.94	14
Diffusion coefficient $h(T)$ (W/(m^2 °C))	5	9.5	11	12	12.5	12.8
Heat conduction coefficient $K(T)$ (W/(m × K))	53.17	51.08	43.96	36.01	34	28
Specific heat $c(T)$ (J/(kg × K))	461	482	557	610	660	770

Table 2
Strain rate properties of the 16 MnR steel

Strain rate $\dot{\varepsilon}$	1×10^{-4}	1×10^{-2}	1×10^{2}	1×10^{3}
Yield stress $\sigma_{s0}(\dot{\varepsilon})$ (MPa)	345	350	550	600

and slowly. Fig. 4 gives the profiles of transient temperatures at different times ($y = 0, z = 150$ mm). After temperature T of the whole weldment approaches to the room temperature $T_0 = 20$ °C, additional 100 steps are calculated for relaxation. Then the residual stress and strain in the plate may be regarded as stable, and correspondingly be used as initial conditions of the following calculations.

Figs. 5 and 6 demonstrates some typical stress distributions along the weld line during cooling. As can be seen from Fig. 5, stress σ_z keeps tensile in the middle of the weld line while compressive near the boundary of plate. The maximum tensile stresses exceed yield stress. The peak values of the calculation results are identical with the numerical results given by Li et al. (2003). In addition, the distributing tendencies of the residual stresses agree with the existing experimental results given by Masubuchi (1980) with regard to the proportional relations between elastic modulus and yield stress. All these prove that the simplification in welding calculation is reasonable and feasible if numerical precision required is not strict. Actually, data at other points are also obtained in the calculation, but detailed process and comparisons are omitted here, since the generation of welding residual stress is not the main concern of this paper.

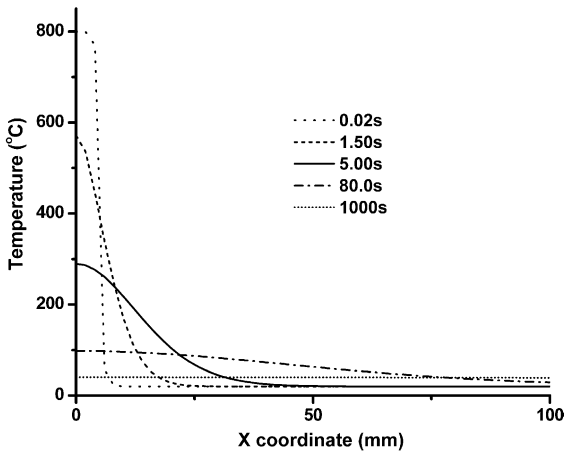

Fig. 4. Temperature evolutions in the course of cooling ($y = 0$, $z = 150$ mm).

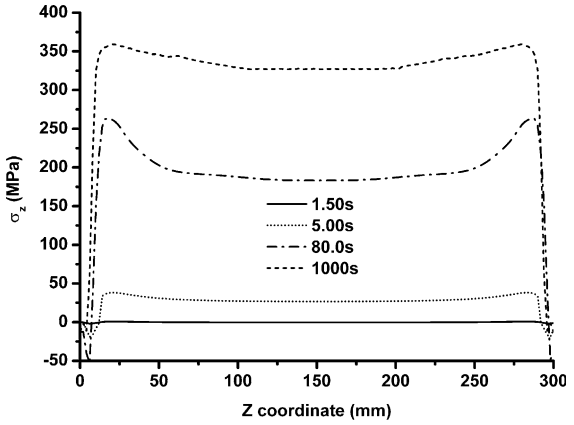

Fig. 5. Evolution of σ_z along the weld line in the course of cooling (x=0, y=0).

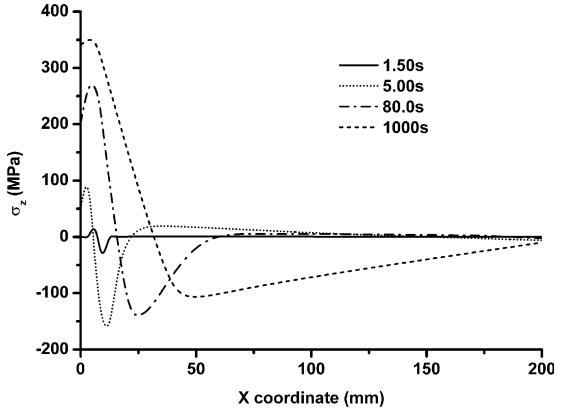

Fig. 6. Evolution of σ_z perpendicular to the weld line in the course of cooling ($y = 0$, $z = 150$ mm).

3.2. Investigation on the course of explosive treatment

Then, stress and strain initiations are obtained from the former analysis. The simulation on stress relief begins at time zero. The explosive loading is simplified as pressure and presented by function $P(x,z,t) = p(x)q(z,t)$, since the action time is extremely short and the thermal effect could be ignored. In detail, sub-functions $q(z,t)$ and $p(t)$ are expressed as follows:

$$q(z,t) = \begin{cases} 0 & t \leqslant z/v_0 \text{ or } t \geqslant z/v_0 + 1.3 \\ \dfrac{t}{z/v_0 + 0.13} & z/v_0 \leqslant t \leqslant z/v_0 + 1.17 \\ 1 & z/v_0 + 1.17 \leqslant t \leqslant z/v_0 + 1.04 \\ \dfrac{t}{z/v_0 + 0.26} & z/v_0 + 1.04 \leqslant t \leqslant z/v_0 + 1.3 \end{cases} \tag{8}$$

$$p(x) = \begin{cases} P_0 F(x) & 0 \leqslant x \leqslant x_0 \\ 0 & x > x_0 \end{cases} \tag{9}$$

where $q(z,t)$ represents the variation with respect to time. $F(x)$ is a function for distribution in x direction. Two forms of $F(x)$ are usually used in case of different detonator strips: for cord shaped detonator, $F(x) = \cos(\frac{\pi}{x_0}x - \frac{\pi}{2})$; for sheet shaped one, $F(x) = 1$. In addition, v_0 is the explosive velocity, P_0 the peak value of loading, x_0 the width of detonator in x direction from the center of the weld line.

The variations of stress and strain fields are surveyed by considering the effect of wave motion, aiming to investigate the mechanism of this technique. When the explosive loading is applied, both of elastic wave and plastic wave are produced, since the elastic limit is exceeded. The speed of elastic wave in 16 MnR steel is $c_0 = 5524$ m/s, while that of plastic wave is much slower and decreases with the increase of strain rates. Fig. 7 presents the variation curves of σ_z with respect to time t at two typical points. Originally, the residual stresses are mainly in form of tensile stress. When the detonators being ignited at time $t = 0$, the explosive loading begins to move along z direction. In this course, compressive waves are produced and thus initial residual stresses are reduced at point I in the weld joint. Afterwards, the compressive wave transforms to tensile wave on the bottom free surface, and then its superimposition with residual tensile stress makes the residual stress increase. On all accounts, after the first round trip, stress value is not decreased but increased, even exceeds the yield stress. Then, after multiple times of wave reflection, accompanied with superimpositions, the final accumulative result is decreased. According to Fig. 7, at time $t = 500$ μs, the oscillation of stress is much weaker. Therefore, the relief of tensile residual stress is assumed to be stable at this time. Another typical point II in heat-affected zone is also marked in Fig. 7. The relieving process of residual stresses at this point is similar with the previous one when the stress wave arrives. So do other points, in fact.

Fig. 8 shows the time histories of plastic strain ε_z^p through the whole process, corresponding to Fig. 7. The plastic strains undergo increasing, decreasing and stable stages. Finally the residual strains are also redistributed and the maximum tensile strains are eliminated. But the variations of plastic strains are little delayed, because of the viscous effect, which is an important factor in the relief of residual strains.

To more extensive range, typical von Mises stress and equivalent plastic strain distributions along the weld line through explosion are given in Figs. 9 and 10. They show the redistribution result of the stresses and strains more explicitly, by comparing the cases before and after the explosion.

3.3. Optimization of the explosive techniques

In engineering, the factors that could affect the reduction efficiency are detonator width x_0, explosive velocity v_0, locations and shapes of detonator strips, maximum loading value P_0, and so on. Investigation on these factors is helpful not only for practical uses, but also for discovering the mechanism of this technique. In the calculation, since σ_z along weld line are the largest stresses in the whole plate, the studies are mainly focused on them.

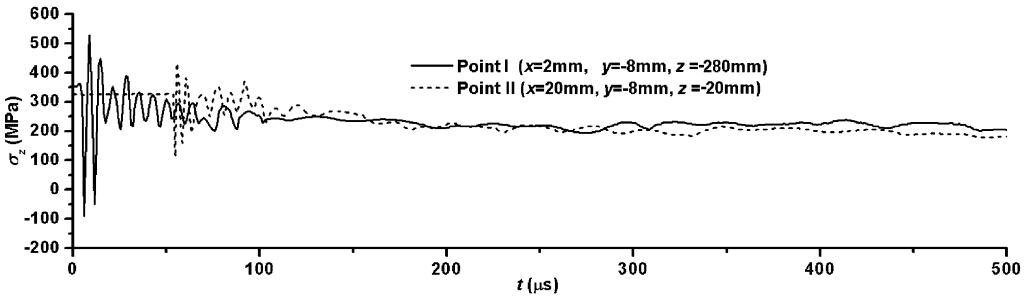

Fig. 7. Variations of σ_z with respect to time t through explosive treatment.

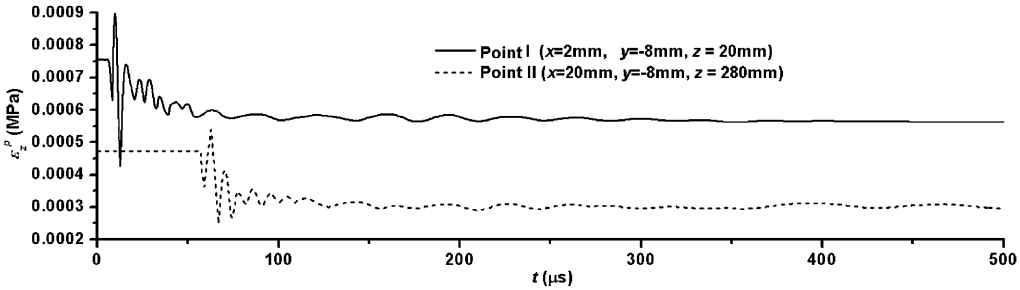

Fig. 8. Variation of plastic strain ε_z^p with respect to time t through explosive treatment.

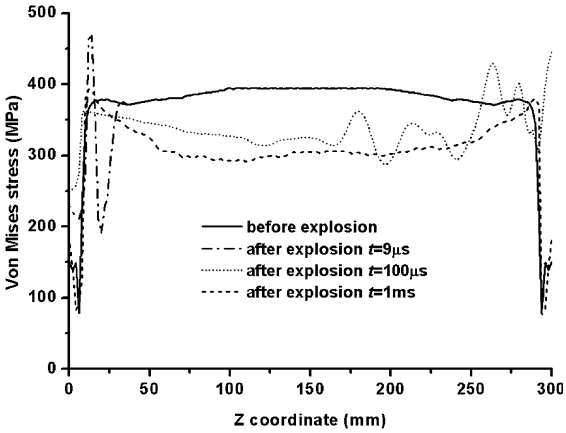

Fig. 9. Variation of von Mises stresses along the weld line through explosive treatment ($x = 0$, $y = 0$).

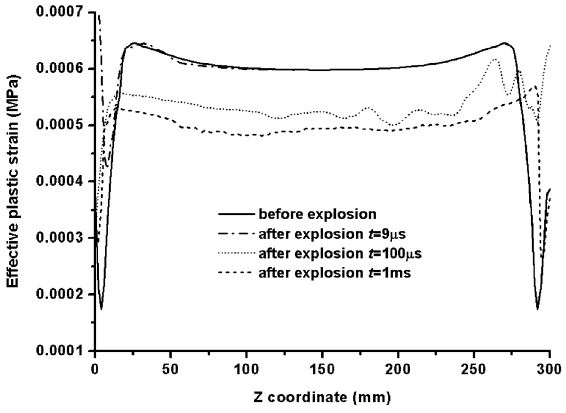

Fig. 10. Variations of equivalent plastic strains along the weld line through explosive treatment ($x = 0$, $y = 0$).

The quantity of detonator strips used affects the quality of explosive treatment directly. Therefore, different widths of detonators are considered here. The detonator strips are laid parallel to the weld line, and same thickness is taken for comparison. The results in Fig. 11 show that the tensile residual stresses

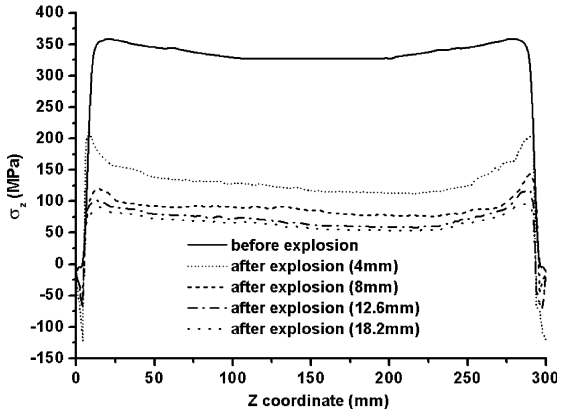

Fig. 11. Comparison of detonator strip widths in explosive treatment ($x = 0$, $y = 0$, $P_0 = 0.5$ GPa, $v = 5400$ m/s, cord shaped detonator).

decrease by a similar tendency. The wider the detonator strip is, the more the residual stresses are reduced. However, it should be noted that the width of detonator x_0 has an upper limit. The excessive detonators beyond this limit are almost useless to the relieving effect, and may cause unnecessary violent stress waves in areas far from the weld line through the explosive course, according to Fig. 7. In this example, the optimal range is 12 mm $\leqslant x_0 \leqslant$ 18 mm, within which σ_z is larger than half of the yield stress, due to the distribution of σ_z in Fig. 6.

Furthermore, considering the practical cases, explosive velocities at four different levels are compared in computation. It is presented in Fig. 12 that with the increase of the explosive velocity, the relieving effect of residual stress is better, if the velocity v_0 is less than 6250 m/s. But if this limit is exceeded, the efficiency is decreased.

Moreover, the amplitude of the loading should be considered in choosing proper detonator amount and species. Here, four kinds of loading values are considered. Fig. 13 indicate that the larger the amplitude of impact loading is, the more the tensile residual stress is reduced. However, too intensive explosion may cause the generation and propagation of micro-cracks in weldment, even result in a fracture of the structure. Therefore, the loading should be confined less than 1GPa in this example.

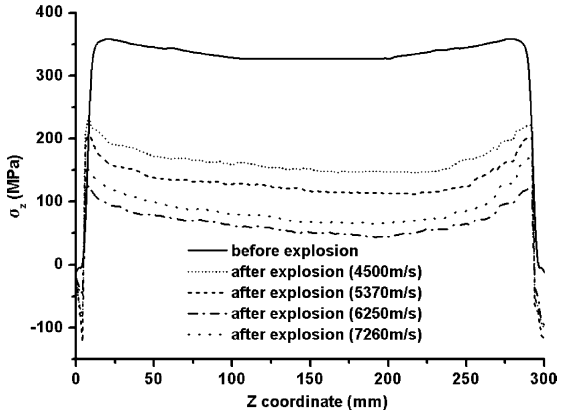

Fig. 12. Comparison of explosive velocities in explosive treatment ($x = 0$, $y = 0$, $P_0 = 0.5$ GPa, $x_0 = 4$ mm, cord shaped detonator).

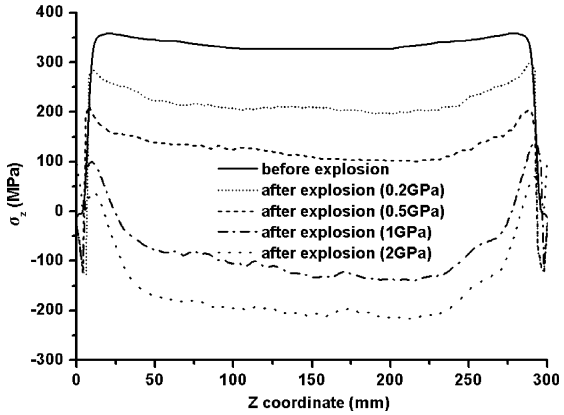

Fig. 13. Comparison of loading amplitudes in explosive treatment ($x = 0$, $y = 0$, $v = 5400$ m/s, $x_0 = 4$ mm, sheet formed detonator).

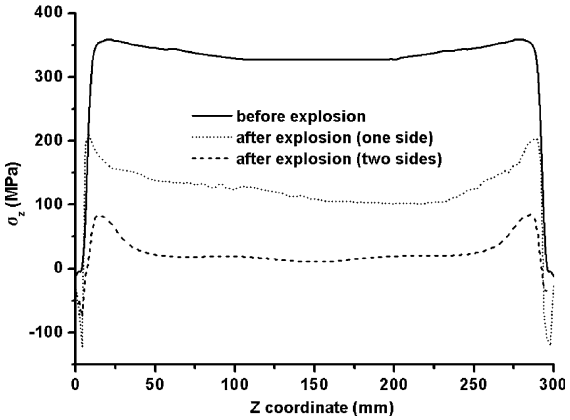

Fig. 14. Comparison of detonator locations in explosive treatment ($x = 0$, $y = 0$, $P_0 = 0.5$ GPa, $v = 5400$ m/s, $x_0 = 4$ mm, sheet shaped detonator).

In practice, the location of detonators on weldment is also an important factor, for example, only on the top surface, or both on top and bottom surfaces. It is proved from comparison in Fig. 14 that explosive treatment on both two sides of the plate would get a more uniform and effective result. Besides, Two forms of detonator strips could also be compared between Figs. 11 and 14 on same conditions ($v = 5400$ m/s, $x_0 = 4$ mm and $P_0 = 0.5$ GPa). The results indicate that the effect from the sheet shaped detonator is better than that of the cord shaped one. The above points agree well with some existing experimental ones (Xie et al., 1995).

4. Experiments

The experiments were performed in 16 MnR steel plates, which were automatically submerged-arc welded. The material parameters are given in Tables 1 and 2, and the dimensions of the specimen are the same as the numerical example shown in Fig. 2.

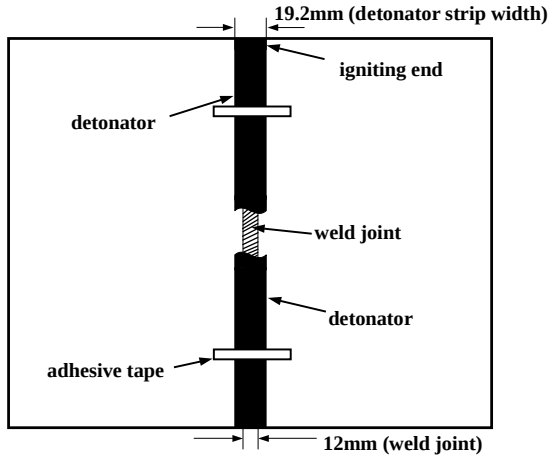

Fig. 15. Layout of the detonator strip.

For the explosive treatment, 19.2 mm wide detonators were stuck on the surface along the weld line as shown in Fig. 15. Between the detonator and the plate, buffers are used to protect the surface of the weldment. In the course of experiment, the detonator was ignited from the origin of the coordinate. The explosive velocity was measured to be 5400 m/s, and the peak value of loading was 500 MPa. Before and after explosive treatment, several points at the top and bottom surface of the plate were chosen to bond strain gages, by which the residual welding stresses were measured by means of blind hole drilling (Masubuchi, 1980).

Figs. 16 and 17 are comparisons of maximum and minimum principal stresses between experimental and numerical results, respectively. After the explosive treatment, the values of the tensile residual stresses decreased explicitly. Even in some areas, the tensile stresses decrease to compressive ones. It can be seen that the numerical results basically coincide with the experimental ones. The error percentage is within the permission of engineering.

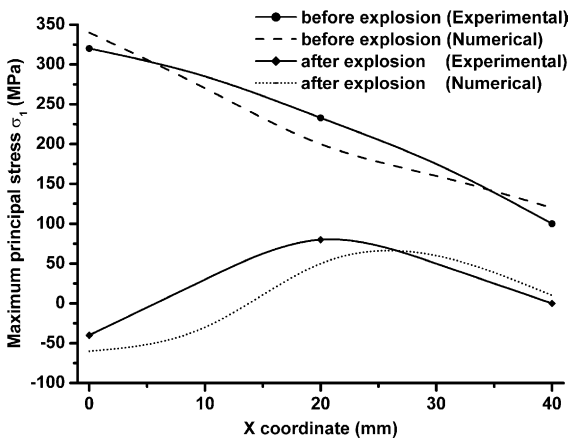

Fig. 16. Comparison of maximum principal stresses σ_1.

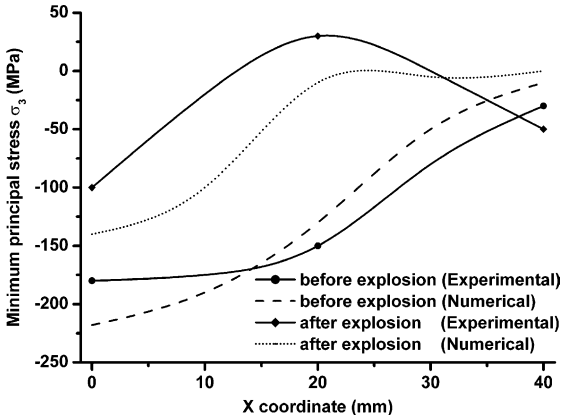

Fig. 17. Comparison of minimum principal stresses σ_3.

5. Conclusions

The whole process of residual stresses generation and reduction in butt-welded steel plates are studied by numerical simulation, theoretical analysis and experimental research. The mechanism of the explosive technique is revealed by tracing the variations of stress wave. Several conclusions are drawn from the investigation.

1. The propagation and interactions of stress waves caused by explosion directly result in redistributions of stress field and plastic strain field in the weldment. The actions of elastic wave, plastic wave and the related viscous effect are crucial for relieving the residual stress in this course.
2. The method using a movable impact to substitute the explosion loading is proved to be effective and reasonable, by comparing the experimental results and the numerical ones. Moreover, the simplifications by adopting indirect method and ignoring heating process in numerical simulation of welding process are feasible, on condition that a thick weldment using multi-pass welding technique is studied and final residual stress and strain fields are mainly concerned.
3. By studying on multiple explosive work conditions, some essential rules on improving the efficiency are obtained as: detonators should put on both sides of the thick plate; the width of detonator should cover the remarkable tensile residual stress region, in which σ_z are larger than half of the yield stress.

Acknowledgements

The authors gratefully acknowledge the support of the National Natural Science Foundation of China (Grant nos. 10025212, 10232040, 10302002 and 10172025).

References

Chadwick, M.D., 1971. Metal. Construction and British welding journal 10 (3), 374.

Editorial board, 1995. Handbook of material data on mechanical engineering (in Chinese). Mechanical Engineering Press, Beijing, China.

Holtzman, A.H., 1966. Process for relieving residual stresses in metals. U.S. Patent No. 3,282,743.
Horioka, M., 1978. Stress relief method by explosives. Japanese Patent No. 53-48188.
Huseby, R.A., 1958. Stress relieving of stainless steels and the associated metallurgy. Welding J. 37 (7), 304–315.
Kudinov, V.M., Petushkov, V.G., 1984. In: 1984 Proc. of the 8th international conference on high energy rate fabrication. San Antonio, Tex., ASME.
Li, M.S., Xie, X. et al., 2003. Numerical simulation of Y-slit type cracking test press (in Chinese). Pressure Vessel Technol. 20 (11), 18–21.
Lin, Y.C., Chou, C.P., 1995. A new technique for reducing the residual stress induced by welding in type 304 stainless steel. J. Mater. Process. Technol. 48, 693–698.
Lu, A.L., Tang, F. et al., 1998. Research on residual-stress reduction by strong pulsed magnetic treatment. J. Mater. Process. Technol. 74, 259–262.
Masubuchi, K., 1980. Analysis of welded structures: residual stresses, distortion, and their consequences. Pergamon press, US.
Schmidt, C., Shockey, D., 1992. Welding Research. Suppl. Welding J. 12, 443s–446s.
Shi, S., Yu, S., 1996. Investigation on the dynamic mechanics properties of 16 MnR steel (in Chinese). J. Ningbo Univ. 9 (3), 72–77.
Shida, Z., et al. 1986. In: Proceedings of the International Symposium on intense dynamic loading and its effects. Beijing, China.
Tall, L., 1964. Residual stresses in welded plate—a theoretical study. Welding J. Suppl., 105–125.
Xie, D., Li, R.F. et al., 1995. Residual stress relief by explosive treatment for weld joints of 16 MnJ heavy-section steel plates (in Chinese). Explos. Shock Waves 15 (1), 76–81.
Yang, Y.S., Lee, S.H., 1997. A study on the mechanical stress relieving in a butt-welded-pipe. Int. J. Press. Vessel Piping 73, 175–182.